

## CBN–Cr/Cr<sub>3</sub>C<sub>2</sub> composite materials: chemical equilibria, XPS investigations

Ewa Benko<sup>a,\*</sup>, Andrzej Wyczesany<sup>b</sup>, A. Bernasik<sup>c</sup>, Tery L. Barr<sup>d</sup>, E. Hoope<sup>d</sup>

<sup>a</sup>*Institute of Metal Cutting, Wroclawska 37A Str., 30-011 Cracow, Poland*

<sup>b</sup>*University of Technology, Warszawska 24 Str., Cracow, Poland*

<sup>c</sup>*Institute of Metallurgy and Materials Science, 25 Reymonta Str., 32-050 Cracow, Poland*

<sup>d</sup>*Materials Department and Laboratory for Surface Studies, University of Wisconsin — Milwaukee, Milwaukee, WI 53201, USA*

Received 2 July 1999; received in revised form 7 July 1999; accepted 13 September 1999

### Abstract

This paper summarizes theoretical and experimental studies of cBN–Cr/Cr<sub>3</sub>C<sub>2</sub> 1:1 and 2:1 molar ratios. From theoretical calculations, it follows that Cr/Cr<sub>3</sub>C<sub>2</sub> react with boron nitride forming one new phase CrB. Experimentally, CBN–Cr/Cr<sub>3</sub>C<sub>2</sub> composites were prepared by high-pressure hot-pressing, and the samples were subsequently heat-treated. The samples after heat treatment were characterized using transmission electron microscopy and X-ray diffraction. Studies of the cBN–metal contact layer presented in this work have been performed using XPS techniques in cooperation with the scientists of the University of Mining and Metallurgy in Cracow, Cracow Technical University as well as the University of Wisconsin — Milwaukee. © 2000 Elsevier Science Ltd and Techna S.r.l. All rights reserved.

**Keywords:** B. Composites; B. Electron microscopy; B. Spectroscopy; B. X-ray methods

### 1. Introduction

Polycrystalline materials produced from cubic boron nitride are widely used in machining due to their unique properties, such as high resistance to oxidation, good thermal conductivity, and chemical inertness to iron and iron alloys [1]. These materials are synthesized in special reactors by high-pressure and high-temperature treatment. The following two procedures are usually applied:

- direct transformation of the hexagonal modification of BN to the cubic one,
- cubic boron nitride sintering with the activation of the sintering process.

The latter procedure is more frequently used. Chemical reactions between the activators and boron nitride occur, resulting in the formation of some new phases. The prediction of the final products of the reactions taking place during the sintering as well as the elucidation of its mechanism is of crucial importance in the selection of the appropriate binding phase.

Titanium, chromium and tantalum and its compounds are most commonly used as binders in sintering technology [2–10].

### 2. Thermochemical analysis of the phenomena taking place in the BN–Cr/Cr<sub>2</sub>C<sub>3</sub> system

For the calculations of the equilibria compositions of the BN-phase systems, the VCS algorithm has been used [11] (the abbreviation originates from the first letters of its authors: Villars, Cruise and Smith). This algorithm belongs to a group of the so-called stoichiometric algorithms, i.e. stoichiometric coefficients of chemical reactions via which the system reaches the equilibrium state are taken into account. The algorithm requires that its user merely lists chemical compounds that can co-exist in the equilibrium state together with their standard thermochemical potentials of formation. Knowledge of the number and types of independent reactions is not necessary for the calculations.

The algorithm is based on minimization of the thermodynamical potential of the whole reacting mixture [Eq. (1)] and this potential is expressed by reaction-extent variables related to the number of mols by Eq. (2).

\* Corresponding author. Fax: +48-1233-9490.

E-mail address: ewa.benko@ios.krakow.pl (E Benko).

$$g = \sum_{i=1}^N n_i \cdot \mu_i = (\min) \quad (1)$$

where  $g$ , thermodynamical potential of the whole reacting system,  $n_i$ , number of mols of the  $i$ -component,  $\mu_i$ , chemical potential of the  $i$ -component,  $N$ , number of components.

$$n_i = n_i^0 + \sum_j^R \gamma_{ij} \cdot \xi_j \quad i, 2, \dots, N' \quad (2)$$

where  $n_i^0$ , starting number of mols of the  $i$ -component,  $\gamma_{ij}$ , stoichiometric coefficient of the  $i$ -component in  $j$ -reaction,  $\xi_j$ , reaction-extent variable of  $j$ -reaction,  $R$ , number of independent reactions,  $N'$ , number of components without the inert ones.

Thus, in the VCS algorithm, the non-linear function of many variables  $f(x)$  is minimized:

$$f(x) = \min$$

where  $x$ , a vector of many variables.

The equilibria compositions in the following systems have been calculated: BN–Cr, BN–Cr<sub>3</sub>C<sub>2</sub>, for the molar ratios of BN: metal equal to 1:1, 1:2 in the wide range of pressure ( $1.3 \times 10^{-3}$ – $1 \times 10^8$  Pa) and temperature (27–2427°C). The data necessary for the calculations (e.g. standard thermodynamical potentials of formation) have been taken from the appropriate tables [11,12].

It has been found from the calculations that all the phases mentioned above react with boron nitride forming new phases.

### 3. Chemical equilibria in the BN–Cr, BN–Cr<sub>3</sub>C<sub>2</sub> systems

#### 3.1. BN–Cr system

For the BN–Cr system in the calculations of chemical equilibria the following components have been taken into account: N<sub>2</sub>(g), B(g), B<sub>2</sub>(g), BN(g), Cr(g), CrN(g), B(l), Cr(s), BN(s), B(s), Cr<sub>2</sub>N(s), CrN(s), CrB(s), Cr<sub>5</sub>B<sub>3</sub>(s), CrB<sub>2</sub>(s).

In the temperature range of 27–727°C, no chemical reactions take place in this system and solid BN and Cr (1 mol each) co-exist in the chemical equilibrium state. At 927°C, under extremely low pressures, Cr<sub>5</sub>B<sub>3</sub> (0.2 mol) and nitrogen (0.3 mol) appear in the system. At 927°C, under the pressure of  $1.3 \times 10^{-3}$  Pa, CrB (0.99 mol) appears in the system. As the temperature increases the pressure range in which the CrB phase exists shifts towards higher values and at 1727°C it reaches the value of  $2\text{--}4 \times 10^4$  Pa. The pressure range in which the solid phases of BN and Cr co-exist gets narrower when the temperature increases and for 27°C it is equal to  $1 \times 10^{-3}$ – $1 \times 10^7$  Pa, whereas for 1727°C it is equal to  $5 \times 10^4$ – $1 \times 10^8$

Pa. There exist such pressure ranges at a given temperature in which only gaseous phases exist in the system.

Chemical equilibria for the BN:Cr molar ratio equal to 2:1 are similar to the system of BN:Cr molar ratio equal to 1:1. Graphical representations of the results of chemical equilibria calculations at 1400°C are shown in Figs. 1 and 2.

#### 3.2. BN–Cr<sub>3</sub>C<sub>2</sub> system

In the calculations of chemical equilibria in this system, the following components have been taken into account: B(g), B<sub>2</sub>(g), N<sub>2</sub>(g), BN(g), Cr(g), C(g), CB(g), CN(g), CN<sub>2</sub>(g), C<sub>2</sub>(g), C<sub>2</sub>N(g), C<sub>2</sub>N<sub>2</sub>(g), C<sub>3</sub>(g), NCN(g), C<sub>4</sub>N<sub>2</sub>(g), C<sub>3</sub>(g), C<sub>4</sub>(g), C<sub>5</sub>(g), B(l), Cr(l), CB<sub>4</sub>(l), CrB<sub>2</sub>(l), Cr<sub>5</sub>B<sub>3</sub>(s), CrB(s), Cr<sub>5</sub>B<sub>3</sub>(s), Cr<sub>2</sub>N(s), Cr(s), Ti(s), BN(s), B(s), C(s), CB<sub>4</sub>(s), Cr<sub>3</sub>C<sub>2</sub>(s), Cr<sub>7</sub>C<sub>3</sub>(s), Cr<sub>2</sub>C<sub>6</sub>(s).

Calculations have been performed for the BN:Cr molar ratios equal to 1:1 and 2:1 in the wide pressure and temperature ranges (from  $1.3 \times 10^{-3}$  to  $1 \times 10^8$  Pa and from 27 to 1727°C). In this system, at temperatures between 27 and 927°C, no chemical reactions occur and

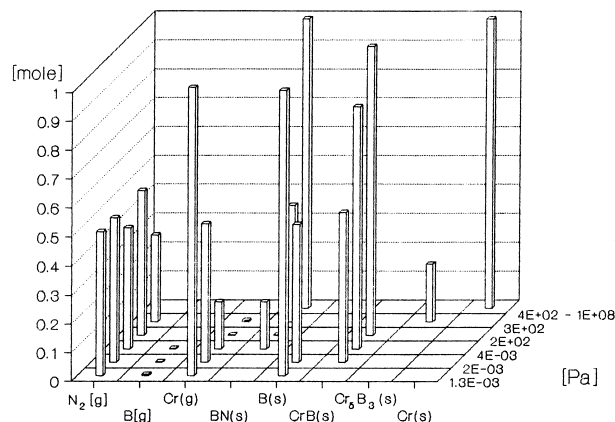


Fig. 1. Chemical equilibria in the BN:Cr = 1:1 system at the temperature of 1400°C.

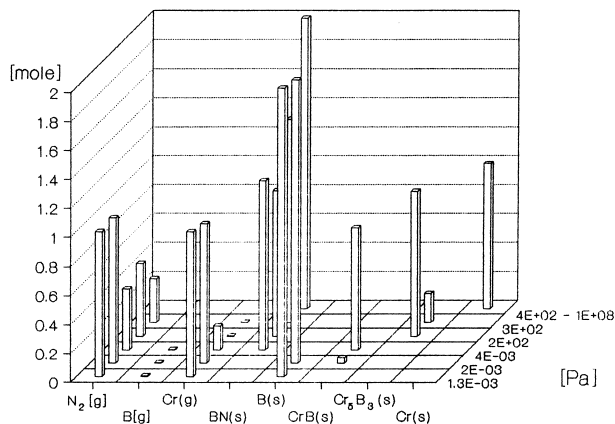


Fig. 2. Chemical equilibria in the BN:Cr = 2:1 system at the temperature of 1400°C.

BN and  $\text{Cr}_3\text{C}_2(\text{s})$  co-exist in the chemical equilibrium state.

At  $1027^\circ\text{C}$ , under extremely low pressure, CrB and C appear as the solid phases in the system in the amounts of 1.0 and 0.67 mol, respectively. As the temperature increases, the pressure range in which these phases exist in the system shifts towards higher pressure values and, at  $1727^\circ\text{C}$ , it is equal to  $1.3 \times 10^{-3}$ – $6 \times 10$  Pa. The pressure range in which BN and  $\text{Cr}_3\text{C}_2$  co-exist in the system gets narrower with the increase of temperature and, at  $1727^\circ\text{C}$ , for BN it is equal to  $7 \times 10$ – $1 \times 10^8$  Pa, whereas for C it is equal to  $1.3 \times 10^{-3}$ – $1 \times 10$  Pa. Starting from  $1027^\circ\text{C}$ , gaseous chromium and nitrogen appear in the system and, at  $1327^\circ\text{C}$ ,  $\text{CB}_4$ . At higher temperatures under low pressures gaseous B, BN, C, CN,  $\text{C}_2$ ,  $\text{C}_2\text{N}$  and  $\text{C}_3$  appear. Chemical equilibria for BN:  $\text{Cr}_3\text{C}_2$  molar ratio equal to 1:1 are similar to the BN:  $\text{Cr}_3\text{C}_2$  molar ratio equal to 2:1. Typical graphical representations of the results of calculations for  $1400^\circ\text{C}$  are shown in Figs. 3 and 4.

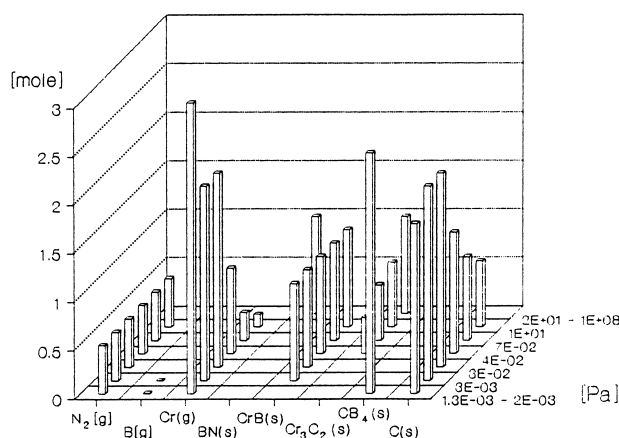


Fig. 3. Chemical equilibria in the BN:  $\text{Cr}_2\text{C}_3 = 1:1$  system at the temperature of  $1400^\circ\text{C}$ .

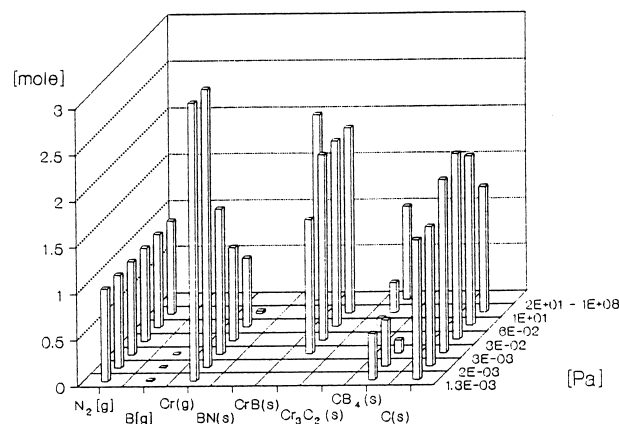


Fig. 4. Chemical equilibria in the BN:  $\text{Cr}_2\text{C}_3\text{r} = 2:1$  system at the temperature of  $1400^\circ\text{C}$ .

#### 4. Identification of the phases formed after sintering of cubic boron nitride with the additions of chromium and chromium carbide

In order to verify the results of theoretical calculations with the experiment model studies have been carried out. In these studies boron nitride of 3/5 and 10/20  $\mu\text{m}$  grain size (produced by de Beers) was sintered with various phases (Cr,  $\text{Cr}_3\text{C}_2$ , produced by MS Stark, 3/5  $\mu\text{m}$  grain size). The mixtures prepared from BN and the components listed above of molar ratios 1:1 and 2:1 have been thermally treated in the pressure range of  $1.3 \times 10^{-3}$ – $1 \times 10^7$  Pa at 1400 and  $1627^\circ\text{C}$  during 2 h. For high-pressure, composite high-pressure press PH0044 equipped with Bridgman cavity chamber (15 mm diameter) was used.

X-ray diffraction studies have been carried out using a Philips 1710 diffractometer. X-ray diffraction pattern identifications were done using a APD-3.5B computer program based on the selected diffraction Data-JCPDS. Filtered  $\text{CuK}_\alpha$ ,  $\text{CoK}_\alpha$ ,  $\text{NiK}_\alpha$  and  $\text{FeK}_\alpha$  radiation were used in the studies.

The results of the studies of the sintered composites can be summarized as follows.

X-ray diffraction studies show good agreement of experimental results with the results of chemical equilibria calculations in the BN–Cr system at temperatures and under pressures used in the experiments. Depending on pressure, either no new phases are formed in the system or a new phase of CrB is formed which corroborates theoretical calculations.

Typical X-ray diffraction patterns of BN:Cr = 1:1 system ( $T = 1400^\circ\text{C}$ ,  $p = 3 \times 10^{-3}$  Pa) are shown in Fig. 5.

The agreement of experimental results with the theoretical ones allows to apply the VCS algorithm in materials science to predict the type and number of new phases formed at given pressure–temperature parameters which, in turn, allows to reduce the number of experiments.

#### 5. TEM studies of cBN sintered with metals, metal carbides

X-ray diffraction studies make it possible to identify the phases existing in the systems. However, they do not give any information on the mutual distributions of these phases. Therefore, it has been necessary to study electron diffraction using the transmission electron microscope which allows study of small areas of the samples.

The sinters in which the BN:  $\text{Cr}_3\text{C}_2$  molar ratio was equal to 1:1 were prepared at  $T = 1750^\circ\text{C}$  under  $p = 7.0$  GPa for 3 min. After high-pressure sintering the samples were additionally thermally treated at  $900^\circ\text{C}$  in vacuum ( $p = 3 \times 10^{-3}$  Pa).

Observations of microstructure of cBN sintered with metals were carried out using a Philips CM20 TWIN (200 kV) transmission electron microscope. Thin films

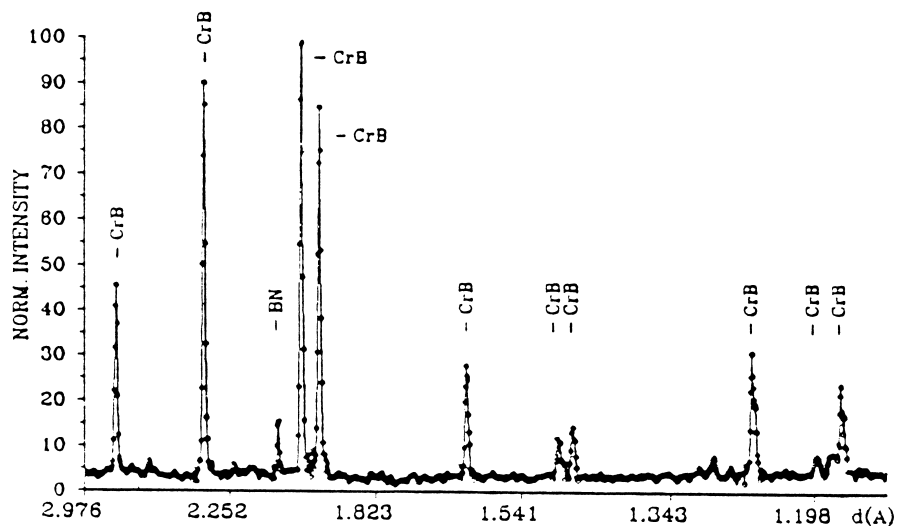


Fig. 5. X-ray diffraction pattern of the BN: = 1:1 system ( $T = 1400^\circ\text{C}$ ,  $p = 3 \times 10^5 \text{ Pa}$ ).

of the samples were obtained using a Gatan 600 Duo-Mill ion drill.

Microstructure of BN sintered with  $\text{Cr}_3\text{C}_2$  immediately after hot-pressing, shown in BN grains structural defects, namely dislocations, and microtwins in boron nitride can be observed.

In the sample after thermal treatment close to the BN surface, fine-crystallites have been observed. Polycrystals of  $\text{Cr}_3\text{C}_2$  have been identified. At the interfaces, one can observe the formation of thin layers of columnar grains and similar crystallographic orientation (Fig. 6). Microanalysis of chemical composition has shown that this layer is formed mainly by chromium boride.

## 6. Studies of the reactions occurring in the BN–Cr, $\text{Cr}_3\text{C}_2$ , systems by X-ray photoelectron spectroscopy

Similarly to auger electron spectroscopy, X-ray photoelectron spectroscopy (XPS) gives important information concerning the chemical composition of the sample studied. By analysis of the chemical shift of a given element, one can obtain important information on its oxidation level as well as the types of bonds that it forms with the surrounding atoms.

XPS is based on the analysis of the energy of photoelectrons emitted by the sample studied excited by the monochromatic radiation. Knowing the kinetic energy of photoelectrons, one can determine the binding energy of the electrons at given atomic levels. Measuring the changes of the electron binding energies, one can conclude upon the chemical and structural changes occurring in the sample.

XPS studies were generally performed on a Hewlett-Packard (HP) 5950A, spectrometer with a high-resolution X-ray monochromator, using an Al  $K_\alpha$  (1476 eV) anode at an irradiation power of 600 W. General

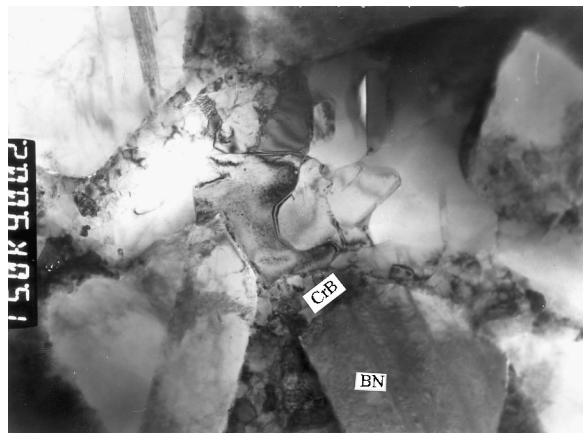


Fig. 6. TEM micrograph showing CrB grains between  $\text{Cr}_2\text{C}_3$  and BN.

calibration produced a binding energy scale specified by the insulating samples removed by a combination of electron flood gun adjustments and fixing the C(1) binding energy of the hydrocarbon part of the adventitious carbon line at 284.6 eV [15]. A curve fitting program of the data was performed after a Shirley background subtraction, using a two-points box curve fitting program with a Gaussian/Lorentzian product function.

Layered samples BN+Cr and BN+ $\text{Cr}_3\text{C}_2$  were prepared using the magnetron sputtering method. The BN plates were used as a substrate corresponding to the material of cutting tools obtaining during direct transformation of hexagonal boron nitride by high-temperature and pressure techniques. The surface was ground by grinding wheels down to grain size 220. Prior to the deposition, BN substrates were cleaned ultrasonically in three steps: acetone, trichloroethylene and propyl alcohol for 15 min each.

The sintered material was thermally treated at  $1400^\circ\text{C}$  for 2 h in vacuum. X-ray diffraction analysis showed

that BN react with Cr and  $\text{Cr}_3\text{C}_2$  forming one new phase: CrB.

The photoelectron peaks for Cr(2p), B(1s), O(1s), N(1s), C(1s) of the investigated samples (BN+Cr/ $\text{Cr}_3\text{C}_2$ ) were examined in order to characterize the chemical interactions between BN and Cr/ $\text{Cr}_3\text{C}_2$ . The best spectrum fitting of the 2pCr peaks was obtained using two doublet lines (2p 3/2 and 2p 1/2) of relative intensity

1:2 and distance 9.7 eV. With this assumption, the spectra of the samples studied were fitted.

The XPS binding energy and relative intensity heat treated BN+Cr/ $\text{Cr}_3\text{C}_2$  systems are shown in Tables 1 and 2 [13–15]. These lines corresponded to Cr-met (metallic), partly oxidized ( $\text{Cr}_2\text{O}_3$ ) and boron partly oxidized ( $\text{B}_2\text{O}_3$ ). The photoelectron peaks for Cr(2p) is different for both samples.

Table 1  
Binding energies and relative peak intensity of compound for Cr–BN deposition system

Element	Binding energy (eV)	Relative peak intensity of elements	Relative intensity of compounds	Compounds
C (1s)	284.6	0.09	0.92	
	288.12		0.08	
B (1s)	187.58	0.05	0.48	CrB <sub>2</sub>
	191.25		0.52	
Cr (2p)	574.39	0.58	0.31	Cr-met, CrB <sub>2</sub>
	576.73		0.69	
O (1s)	531.45	0.25		
N (1s)	398.36	0.03		

Table 2  
Binding energies and relative peak intensity of compound for  $\text{Cr}_2\text{C}_3$ –BN deposition system

Element	Binding energy (eV)	Relative peak intensity of elements	Relative peak intensity of compounds	Compounds
C (1s)	284.6	0.11	0.87	
	287.78		0.13	
B (1s)	187.83	0.11	0.75	CrB <sub>2</sub>
	191.89		0.25	
Cr (2p)	574.44	0.50	0.24	Cr-met, CrB <sub>2</sub>
	577.18		0.76	
O (1s)	531.68	0.25		
N (1s)	398.91	0.03		

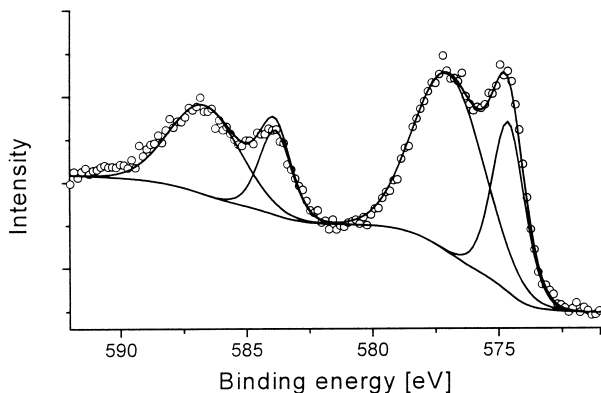


Fig. 7. Cr (2p) photoelectron spectrum of the BN–Cr sample.

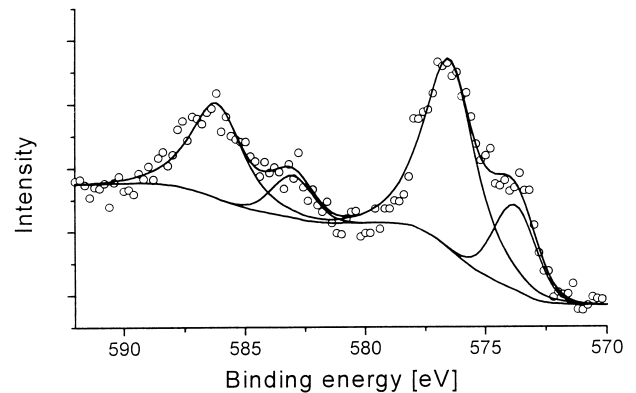


Fig. 8. Cr (2p) photoelectron spectrum of the BN– $\text{Cr}_2\text{C}_3$  sample.

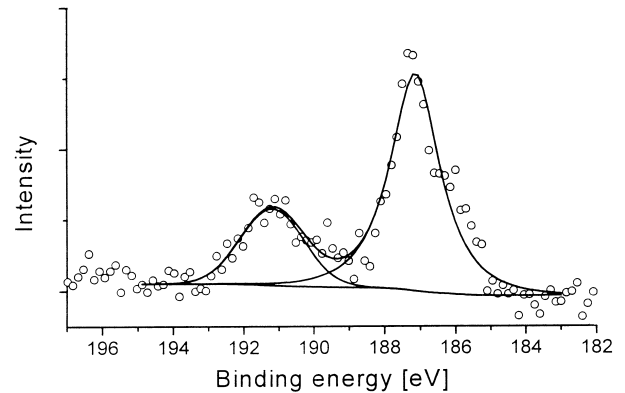


Fig. 9. B (1s) photoelectron spectrum of the BN–Cr sample.

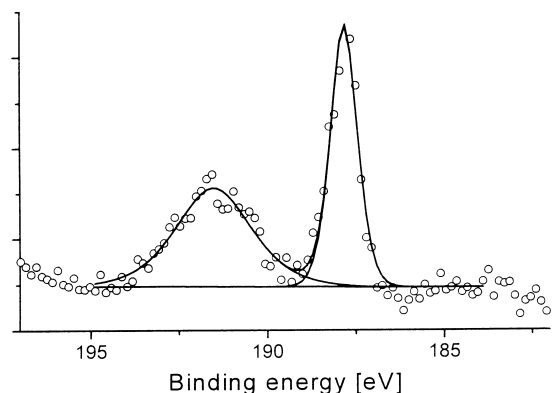


Fig. 10. B (1s) photoelectron spectrum of the BN– $\text{Cr}_2\text{C}_3$  sample.

XPS analysis thermal-treated (at 1400°C for 2 h) samples BN+Cr and BN+Cr<sub>3</sub>C<sub>2</sub> indicated also the formation of CrB on the surface of Cr and Cr<sub>3</sub>C<sub>2</sub> coated BN. The highest intensity of B1s line was observed for sample CrC+BN and highest value of the CrB by smaller value of B–O. This sample also provided the highest observed value of Cr-met (Figs. 7–10)

## 7. Conclusion

The results of X-ray diffraction studies unequivocally indicate good agreement of the experimental data with the calculated equilibrium composition for both molar ratios studied at least in the temperature and pressure ranges investigated experimentally. Only one new phase was detected, as predicted by the VCS method. The calculated and experimental contents of coexisting phases agree within the experimental error. Such calculations are extremely important from the technological point of view since they facilitate the engineering of new materials with desired properties.

XRD revealed the presence of new-phase CrB in the Cr–BN and Cr<sub>3</sub>C<sub>2</sub>–BN. TEM observation exhibited a compact structure in the Cr<sub>3</sub>C<sub>2</sub>–BN system showing the formation of CrB at the Cr<sub>3</sub>C<sub>2</sub>–BN interface. XPS analysis of 1400°C treated Cr–BN and Cr<sub>3</sub>C<sub>2</sub>–BN samples showed CrB on the surface. The thermal treatment does play an important role in the chemical interaction in present systems. XPS data indicated the formation of chromium boride at the surface of the both samples.

## Acknowledgements

This study is based on the work sponsored by the Polish–American Maria Skłodowska-Curie Joint II grant in cooperation with Ministry of Industry and Office of International Affairs National Institute of Standards and Technology under project MP/NIST-96-261.

## References

- [1] Venezar i inni: Polucenie i primienienie sverhtverdyh materialov. ISM, Kiev, USSR, 1986.
- [2] F.P. Bundy, H.P. Bovenkerk, H.M. Strong, R.H. Wentorf, J. Chem. Phys. 35 (2) (1961) 394.
- [3] F.P. Bundy, J. Chem. Phys. 38 (3) (1963) 618–630.
- [4] F.P. Bundy, J. Chem. Phys. 38 (3) (1963) 631–643.
- [5] R. Berman, F. Simon, Z. Electrochem. 55 (5) (1955) 333–338.
- [6] F.R. Corrigan, F.P. Bundy, J. Chem. Phys. 63 (9) (1975) 3812.
- [7] V.L. Solozhenko, Doklady Phys. Chem. AN SSSR 301 (1) (1988) 147–149.
- [8] V.L. Solozhenko, High Press. Res. 7 (1991) 201.
- [9] V.L. Solozhenko, Thermochim. Acta 218 (1993) 201.
- [10] V.L. Solozhenko, Diamond and Related Materials 4 (1994) 1–4.
- [11] W.P. Smith, R.W. Missen, Chemical Reaction Equilibrium Analysis: Theory and Algorithms, Wiley, New York, 1982.
- [12] D.R. Stull, M. Prophet, IANAF Thermochemical Tables, 2nd Edition, NSRDS-NBS37, National Bureau of Standards, Washington, DC, 1971.
- [13] T.L. Barr, Modern ESCA, CRC Press, Boca Raton, FL, 1994.
- [14] D. Wagner, D.M. Bickham, NIST X-ray Photoelectron Spectroscopy Database. National Institute of Standards and Technology, Gaithersburg, MD 20899, October 1989.
- [15] T.L. Barr, S. Seal, J. Vac. Sci. Technol. A 13 (1995) 1239.